Stark effect dependence on hydrogenic impurity position in a cubic quantum box

Carlos I. Mendoza
Instituto de Investigaciones en Materiales, Universidad Nacional Autónoma de México, Apartado Postal 70-360, 04510 México, Distrito Federal, Mexico

G. J. Vazquez and M. del Castillo-Mussot
Instituto de Física, Universidad Nacional Autónoma de México, Apartado Postal 20-364, 01000 México, Distrito Federal, Mexico

H. Spector
Department of Physics, Illinois Institute of Technology, Chicago, Illinois 60616, USA
(Received 26 November 2003; revised manuscript received 24 September 2004; published 28 February 2005)

We carry out a detailed variational calculation of the binding energies of hydrogenic impurities in a cubic quantum box as a function of both the impurity position and an applied electric field. It is found that the binding energy of the impurities is highly dependent on the impurity position, and the electric field splits the energy of impurities on points of the box which are equivalent in the absence of the electric field. When the impurity is located at the upper half of the cube and the field pushes the particle downwards, then the binding energy decreases, whereas the Stark shift exhibits a minimum.

DOI: 10.1103/PhysRevB.71.075330 PACS number(s): 73.21.−b

I. INTRODUCTION

Man-made low-dimensional solids yield challenges in microstructure materials science. Size quantization in man-made semiconductor structures leads to exciting electronic properties which are important for fundamental physics and for the development of device concepts. Fundamental research as well as device applications based on these low-dimensional semiconductor structures require methods to fabricate the structures and to control their geometrical size on the nanometer scale in a reproducible manner. Typical examples of low-dimensional systems are quasi-two-dimensional quantum layers (QL), quasi-one-dimensional quantum wires (QW), and quasi-zero-dimensional structures such as quantum dots (QD). In QD or quantum boxes, the carriers are confined in their motion along all three directions. There has been much work, both theoretical and experimental on the Stark effect in QL (Refs. 1–7) and QW (Refs. 8–13). Energy levels and oscillator strengths for transitions between the lowest states of an acceptor in a QD of finite potential barrier have been computed.[14]

There has also been much work on the binding energy of hydrogenic impurities in spherical QDs.[15–21] Within the perturbation method, the comparison of the field-induced shift in ground levels of spherical and a cubic QD has proved a spherical QD to be more sensitive to an applied field than a quantum cube.[22] Both electric and magnetic field effects of shallow donor impurities have been theoretically investigated in Refs. 23 and 24. In Ref. 23 cylindrical QDs were modeled by superposing a lateral parabolic potential and a square-well potential in the z direction. In Ref. 24 the confinement in the spherical QD is parabolic, and the impurity interaction was treated as a perturbation, which is a good approach as long as the QD radius is much less than the effective Bohr radius. Ribeiro and Latge[25] calculated the donor binding energies of impurities states of a hydrogenic impurity in a QD without an electric field following a variational procedure. In their results, the emphasis is placed on the dependence of the binding energy on the volume of the QD and on the impurity position. On the other hand, excitonic wave function, the corresponding correlation energy, exchange energy, and oscillator strength in a cubic QD were calculated following a variational procedure[26] similar to that of Ref. 25. In Ref. 26 they were able to reduce all the sixfold integrals to threefold integrals with a change of variables which shortens tremendously the computer calculation. Lozano-Cetina and Porras-Montenegro[27] performed a variational calculation of a cubic quantum box with a hydrogenic impurity located along one symmetry direction. Here we employ this model to explore the binding energy and the Stark effect when the impurity is located at many representative positions of the cube. A brief account of the present work is given in Ref. 28.

II. CALCULATION

The Hamiltonian of an electron in a quantum box in the presence of an impurity and an electric field applied along an axis of symmetry of the box is

$$H = \frac{p^2}{2m^*} - \frac{e^2}{\kappa\sqrt{(x-x_i)^2+(y-y_i)^2+(z-z_i)^2}} + |e|Fz + V_c(x,y,z), \tag{1}$$

where $F>0$ is the electric field, m^* and $|e|$ are the electron's effective mass and charge, respectively, κ is the dielectric constant, and $V_c(x,y,z)$ is the confining potential which takes the value zero in the interior of the quantum box and it is infinity otherwise.

We will use the variational ground state wave function proposed in Ref. 27,

$$\Psi(x,y,z) = N\cos\left(\frac{\pi x}{L_x}\right)\cos\left(\frac{\pi y}{L_y}\right) \times\cos\left(\frac{\pi z}{L_z}\right)\left[\mathrm{Bi}(\tilde{z}) - \frac{\mathrm{Bi}(\xi_L)}{\mathrm{Ai}(\xi_L)}\mathrm{Ai}(\tilde{z})\right] \times \exp[-\alpha\sqrt{(x-x_i)^2+(y-y_i)^2+(z-z_i)^2}], \quad (2)$$

for $x<|L_x/2|$, $y<|L_y/2|$, $z<|L_z/2|$, with the parameter $\tilde{z}$ given by

$$\tilde{z} = \left(\frac{2m^*eF}{\hbar^2}\right)^{-2/3}\left[\frac{2m^*}{\hbar^2}(|e|Fz - E_0) + (K_x^2 + K_y^2)\right], \quad (3)$$

and $K_x=\pi/L_x$, $K_y=\pi/L_y$, $\xi_L=\tilde{z}(z=-L_z/2)$, and $\xi_R=\tilde{z}(z=L_z/2)$.

In these equations, x_i, y_i, and z_i are the coordinates of the impurity in the quantum box, $\mathrm{Bi}(\tilde{z})$ and $\mathrm{Ai}(\tilde{z})$ are the Airy functions, and N is the normalization constant. The exponential term in Eq. (2) accounts for the presence of the hydrogenic impurity, with α as a variational parameter. We would like to point out that this one-parameter variational wave function is accurate for hydrogenic impurities,[29] and it is very simple to provide physical insight into the problem. In this way, this calculation can serve as a guide for both experimentalists and theoreticians.

We calculate $E=\langle\Psi|H|\Psi\rangle$ by minimizing it with respect to α and define the binding energy of the impurity ε_b as

$$\varepsilon_b = E_0 - \langle\Psi|H|\Psi\rangle, \quad (4)$$

where E_0 is the ground energy of the QD in the absence of the impurity, calculated by means of the equation $\mathrm{Ai}(\xi_R)\mathrm{Bi}(\xi_L)=\mathrm{Ai}(\xi_L)\mathrm{Bi}(\xi_R)$. For a cubic quantum box, we have $L_x=L_y=L_z=L$.

III. RESULTS

All the results will be presented in reduced atomic units (a.u.*) which correspond to a length unit of an effective Bohr radius, $a^*=\hbar^2\varepsilon_0/m^*e^2$, and an effective Rydberg, $R^*=m^*e^4/2\hbar^2\kappa^2$. For donor impurities in a GaAs QD of side $L=a^*$ these units correspond to $a^*\simeq 100$ Å and $R^*\simeq 5.72$ meV. In Fig. 1, we present the binding energy of hydrogenic impurities in a cubic GaAs quantum box of side 10 nm as a function of the impurity position inside the box considering different symmetry lines within the box: along the cube diagonal (curve *A*), along the diagonal of the square cross section at $z_i=0$ (curve *B*), along the diagonal of the cube face ($z_i=L/2$) with $x_i=y_i$ (curve *C*), along the cube face ($z_i=L/2$) with $y_i=0$ and x_i varying from 0 to $L/2$ (curve *D*), along the vertical axis with $x_i=y_i=0$ and z_i varying from 0 to $L/2$ (curve *E*), and along the cube edge with $z_i=x_i=L/2$ and y_i varying from 0 to $L/2$ (curve *F*). The figure shows that the binding energy decreases as the impurity gets further from the center of the box and along those directions which pass through the center of the box (curves *A*, *B*, and *E*). For these curves, the binding energy is higher at $x_i=0$ than for those directions which pass through the center of the face of the box (curves *C* and *D*) which in turn have higher energy than that passing through the edges of the cube (curve *F*).

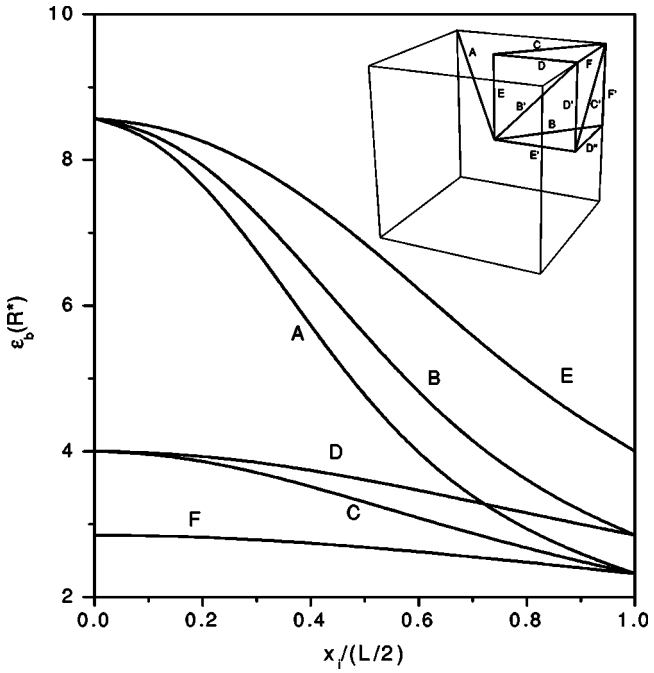

FIG. 1. Binding energy of hydrogenic impurities ε_b in a cubic GaAs QD of side 10 nm as a function of the impurity position. We consider different symmetry lines and no electric field is applied. In the inset we show the cubic QD with symmetry lines—along the cube diagonal (curve *A*), along the diagonal of the square cross section at $z_i=0$ (curve *B*), along the diagonal of the cube face with $z_i=L/2$ with $x_i=y_i$ (curve *C*), along the cube face with $z_i=L/2$, $y_i=0$ and x_i varying from 0 to $L/2$ (curve *D*), along the vertical axis with $x_i=y_i=0$ and z_i varying from 0 to $L/2$ (curve *E*), and along the cube edge with $z_i=x_i=L/2$ and y_i varying from 0 to $L/2$ (curve *F*). We also indicate equivalent directions with the same letters but one or two primes. These directions cease to be equivalent under an applied electric field along the *z* direction.

The binding energy of the hydrogenic impurities is shown in Fig. 2 as a function of the impurity position inside the box considering different symmetry lines within the box and for an electric field $F=60(|e|/2\kappa a^{*2})$. According to the Hamiltonian, the direction of the field was chosen to push the particle downwards. In this way if the impurity is located in the upper half of the cube, then an interesting competing effect is originated between the applied electric Stark field and the impurity field, as will be shown later on. Six additional symmetry lines in addition to the curves shown by curves *A*, *B*, *C*, *D*, *E*, and *F* are shown here: along the diagonal of the square cross section at $y_i=0$ (curve B'), along the diagonal of the cube face ($x_i=L/2$) with $z_i=y_i$ (curve C'), along the cube face ($x_i=L/2$) with $y_i=0$ and z_i varying from 0 to $L/2$ (curve D') and along the cube face ($x_i=L/2$) with $z_i=0$ and y_i varying from 0 to $L/2$ (curve D''), along the horizontal axis with $z_i=y_i=0$ and x_i varying from 0 to $L/2$ (curve E'), and along the cube edge ($x_i=y_i=L/2$ and z_i varying from 0 to $L/2$) (curve F'). In all cases, the binding energy decreases as the location of the impurity moves further from the center of the box. The binding energy is higher at the center of the box

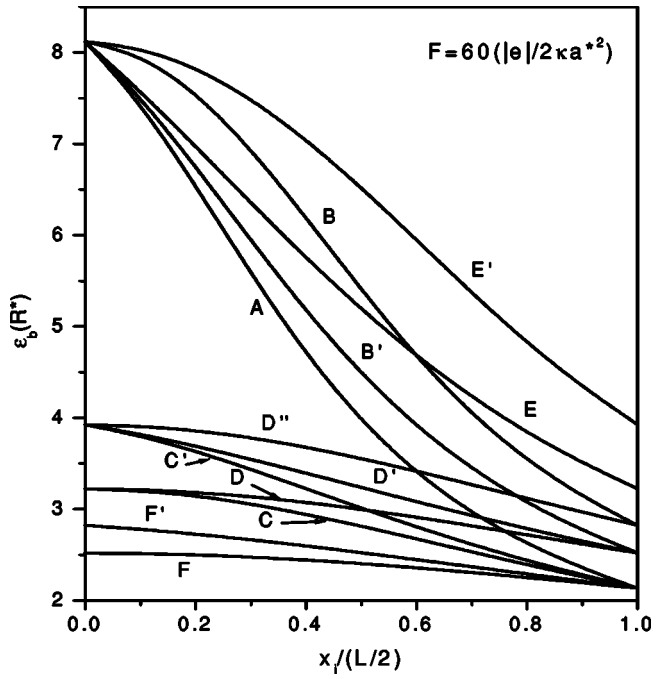

FIG. 2. Same as Fig. 1 but with electric field $F=60$ ($|e|/2\kappa a^{*2}$). Six additional symmetry lines in addition to the curves shown by A, B, C, D, E, and F are shown here—along the diagonal of the square cross section at $y_i=0$ (curve B'), along the diagonal of the cube face ($x_i=L/2$) with $z_i=y_i$ (curve C'), along the cube face ($x_i=L/2$) with $y_i=0$ and z_i varying from 0 to $L/2$ (curve D'), and along the cube face ($x_i=L/2$) with $z_i=0$ and y_i varying from 0 to $L/2$ (curve D''), along the horizontal axis with $z_i=y_i=0$ and x_i varying from 0 to $L/2$ (curve E'), and along the cube edge ($x_i=y_i=L/2$ and z_i varying from 0 to $L/2$) (curve F').

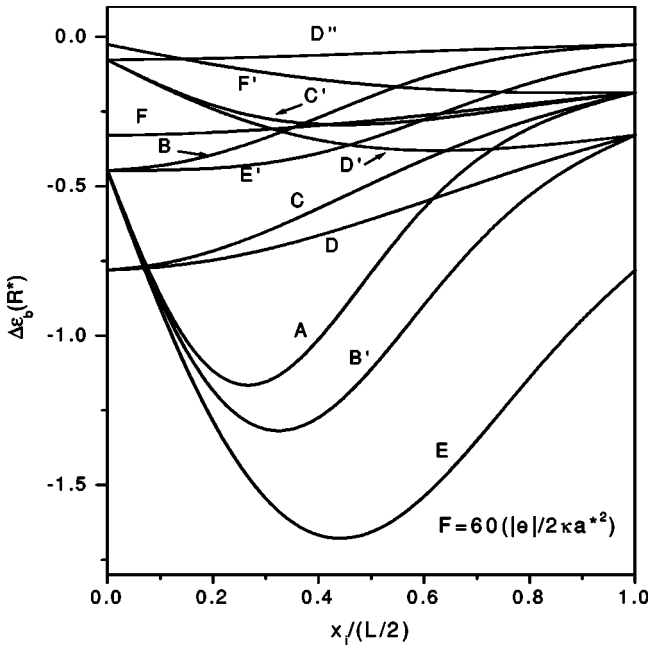

FIG. 3. Differences of energies $\Delta\varepsilon_b$ (or Stark shifts) of Figs. 1 and 2 where we subtract ε_b in Fig. 1 from ε_b in Fig. 2 along the equivalent symmetry lines.

than it is at the center of the faces of the box. Also, although the binding energy along curves B and B' are identical in the absence of the electric field, they are split by the electric field. The same applies for the curves C and C', the curves D, D', and D'', the curves E and E', and the curves F and F'. Therefore, as expected, the degeneracy of the binding energy of hydrogenic impurities located at points of the box which are equivalent in the absence of the electric field are removed by its presence.

The corresponding Stark shift $\Delta\varepsilon_b$ is shown in Fig. 3 and is obtained by substracting ε_b of Fig. 1 from ε_b of Fig. 2 along the equivalent symmetry lines. Only those symmetry lines that have a vertical component (A, B', C', D', E, and F') exhibit a minimum in $\Delta\varepsilon_b(F)$. To explain this behavior, we recall that due to the electric field, most of the particle probability density is located in the lower part of the box, lowering the energy due to the interaction with the field. Then, when the impurity is moved upwards (with an increasing vertical component), the Coulomb interaction energy between the impurity and the particle, which is always negative, increases. These two competing effects give rise to the minimum in $\Delta\varepsilon_b$.

In Fig. 4, ε_b is shown as a function of the electric field for the impurity located at various positions in the box (points a, b, b', b'', c, c', and d) which are shown in the inset of the figure. The binding energy is largest when the impurity is located at the center of the box (point a). Also, impurities located on the center of the cube faces (points b, b', and b'') have the same binding energy in the absence of the electric field but have different energies in the presence of the field. Similarly, impurities located on the center of the cube edges (points c and c') have the same binding energy in the absence of the field but different energies in the presence of the

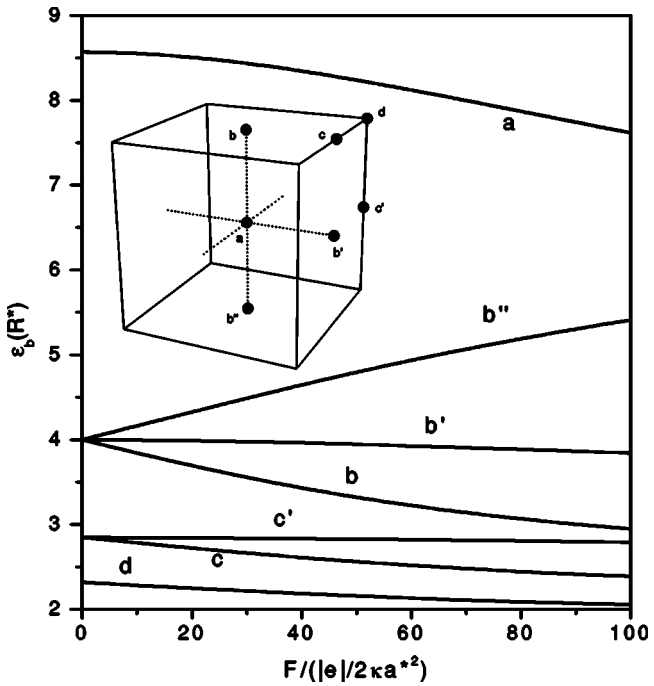

FIG. 4. ε_b is shown as a function of the electric field for the impurity located at various positions in the QD (points a, b, b', b'', c, c', and d) which are shown in the inset.

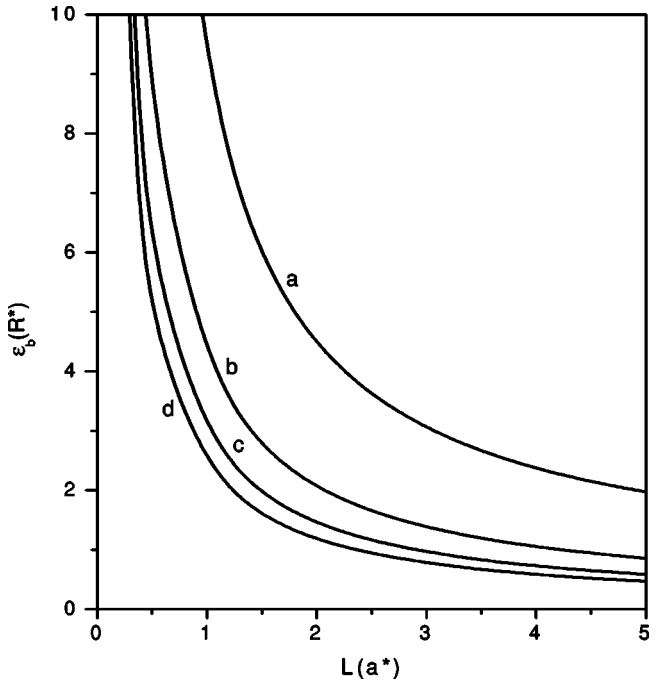

FIG. 5. ε_b at positions a, b, c, and d as a function of length L.

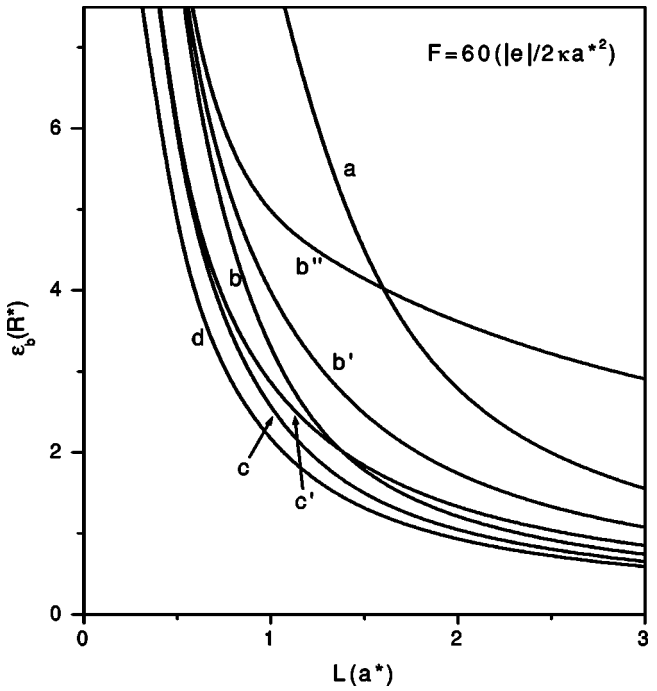

FIG. 6. Same as Fig. 5 but with $F=60$ ($|e|/2\kappa a^{*2}$) and including additional points b', b'', and c'. Energy splittings are shown.

field. For impurities located at any of these points, the binding energy increases with the electric field. The binding energy is lowest when the impurity is located at the corner of the cube (point d).

We show in Fig. 5 the binding energy in positions a, b, c, and d as a function of the cube size L. As expected, the binding energy decreases with increasing L. Finally, Fig. 6 is the same as Fig. 5, but with an electric field $F=60(|e|/2\kappa a^{*2})$. Here, additional points b', b'', and c' are considered.

IV. DISCUSSION AND CONCLUSIONS

Our results qualitatively agree with those of Ref. 23 for cylindrical QDs (in which the impurity position is only changed along the cylinder axis) in the sense that ε_b increases when the electron is pushed by the field towards the impurity as shown in Fig. 4 of Ref. 23. (Incidently, notice that the zero field case in their figure caption is incorrectly labeled by dotted curves, which contradicts the labels inside the figure.) The main differences between that work[23] and ours, however, are the following. First, our QD is a cube with infinite hard walls and theirs is a cylindrical QD with a lateral parabolic confinement. Second, although in the z direction their confinement is the same as ours, in the lateral directions their confinement is very weak, leading to smaller binding energies as compared to ours. Finally, the range of Stark-field intensities is wider in our work. It is important to mention that in Ref. 27 the authors calculated the binding energy for only one case: when the impurity is moved from the center of the cube along the z direction. Our calculation is the first one to show the splittings of the binding energy along the symmetry lines due to the electric field.

On the other hand, due to confinement, the electron density probability must vanish at the walls. Therefore, when the impurity is located at the wall, the wave function in regions closer to the impurity (which more contributes to the increase of the binding energy) suffers the wall constrictions and has to vanish rapidly. For instance, for $F=0$ we observe that ε_b is larger when the impurity position is farther from the corners. Thus, $\varepsilon_b(a)>\varepsilon_b(b)>\varepsilon_b(c)>\varepsilon_b(d)$. Also, it seems clear that ε_b decreases as the electric field increases if the impurity is located in the upper half of the QD. This is due to the fact that the applied electric field tends to push the electron far from the impurity, because for $z>0$ we have that $|e|Fz>0$. Conversely, if the impurity is located in the lower part of the QD, the binding energy increases because the field tends to push the electron closer to the impurity. It can also be noticed that the binding energy ε_b decreases more for impurity positions, with $z>0$ farther from the bottom of the cube. For example, $\varepsilon_b(b)>\varepsilon_b(b')$ for all $F>0$.

In summary, we have analyzed the dependence on an applied electric field of the binding energy of impurities at different positions in a cubic QD. We showed that this energy strongly depends on the position of the impurity; it increases its value for impurity positions in the lower half of the cube and conversely for the upper half positions. Finally, we calculated the binding energy splittings for points of the box which are equivalent in the absence of the electric field. We hope that the detailed analysis of the combined effects of confinement, electric field, and impurity position will stimulate further research on analogous systems.

ACKNOWLEDGMENTS

This work was supported in part by Grant No. DGAPA-UNAM IN106201 and CONACyT (México) Grant No. 32293-E.

[1] J. A. Brum and G. Bastard, Phys. Rev. B **31**, 3893 (1985).
[2] G. Bastard, E. E. Mendez, L. L. Chang, and L. Esaki, Phys. Rev. B **28**, 3241 (1983).
[3] D. A. B. Miller, D. S. Chemla, T. C. Damen, A. C. Gossard, W. Wiegmann, T. H. Wood, and C. A. Burrus, Phys. Rev. B **32**, 1043 (1985).
[4] M. Matsuura and T. Kamizato, Phys. Rev. B **33**, 8385 (1986).
[5] Y. P. Feng and H. N. Spector, Phys. Rev. B **48**, 1963 (1993).
[6] Y. P. Feng and H. N. Spector, Phys. Status Solidi B **190**, 211 (1995).
[7] Y. P. Feng, H. S. Tan, and H. N. Spector, Superlattices Microstruct. **17**, 267 (1995).
[8] G. J. Vázquez, M. del Castillo-Mussot, and H. N. Spector, Phys. Status Solidi B **240**, 561 (2003).
[9] M. A. Dupertuis, E. Martinet, H. Weman, and E. Kapon, Europhys. Lett. **44**, 759 (1998).
[10] D. Huynh Thanh and D. B. Tran Thoai, Physica B **293**, 1 (2000).
[11] S. Benner and H. Haug, Phys. Rev. B **47**, 15 750 (1993).
[12] T. Arakawa, Y. Kato, F. Sogawa, and Y. Arakawa, Appl. Phys. Lett. **70**, 646 (1997).
[13] R. Rinaldi, R. Cingolani, L. DeCaro, M. Lomascolo, M. Didio, L. Tapfer, U. Marti, and F. K. Reinhart, J. Opt. Soc. Am. B **13**, 1031 (1996).
[14] P. Janiszewski and M. Suffczynski, Acta Phys. Pol. A **88**, 1171 (1995).
[15] D. S. Chuu, C. M. Hsiao, and W. N. Mei, Phys. Rev. B **46**, 3898 (1992).
[16] J. L. Zhu, Phys. Rev. B **39**, 8780 (1989).
[17] N. Porras-Montenegro and S. T. Perez-Merchancano, Phys. Rev. B **46**, 9780 (1992).
[18] N. Porras-Montenegro, S. T. Perez-Merchancano, and A. Latge, J. Appl. Phys. **74**, 7652 (1993).
[19] C. C. Yang, L. C. Liu, and S. H. Chang, Phys. Rev. B **58**, 1954 (1998).
[20] J. L. Zhu, J. J. Xiong, and B. L. Gu, Phys. Rev. B **41**, 6001 (1990).
[21] J. L. Zhu and Xi Chen, Phys. Rev. B **50**, 4497 (1994).
[22] C. Bose, Indian J. Phys., A **71A**, 293 (1997).
[23] F. J. Ribeiro, A. Latge, M. Pacheco, and Z. Barticevic, J. Appl. Phys. **82**, 270 (1997).
[24] K. D. Zhu and S. W. Gu, Phys. Lett. A **181**, 465 (1993).
[25] F. J. Ribeiro and A. Latge, Phys. Rev. B **50**, 4913 (1994).
[26] R. Romestain and G. Fishman, Phys. Rev. B **49**, 1774 (1994).
[27] J. C. Lozano-Cetina and N. Porras-Montenegro, Phys. Status Solidi B **210**, 717 (1998).
[28] C. I. Mendoza, G. J. Vázquez, M. del Castillo-Mussot, and H. N. Spector, in Proceedings of the Congreso Latinoamericano de Ciencias de Superficies y sus Aplicaciones (CLACSA), Pucón, Chile, 2003 [Phys. Status Solidi C **1**, S74 (2004)].
[29] A. M. Stoneham, *Theory of Defects in Solids: Electronic Structure of Defects in Insulators and Semiconductors* (Oxford University Press, Oxford, 1975), Table 6.1.